Supporting Information

Magnetoelectric behavior of 0-3 Co/$BaTiO_3$-Composites

Toni Buttlar and Stefan G. Ebbinghaus*

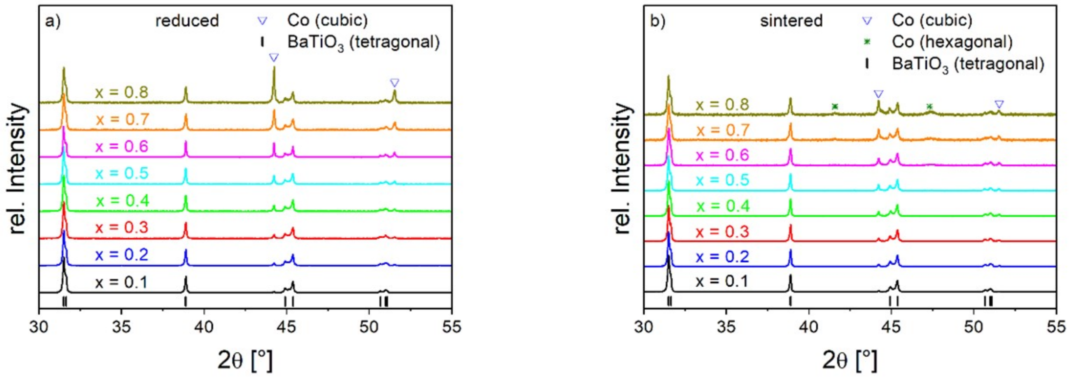

Figure S1: XRD patterns of all $Co_x/(BaTiO_3)_{1-x}$ composites after reduction in forming gas at 1073 K for 2 h (a) and after sintering in nitrogen at 1623 K for 2 h with carbon as oxygen getter (b).

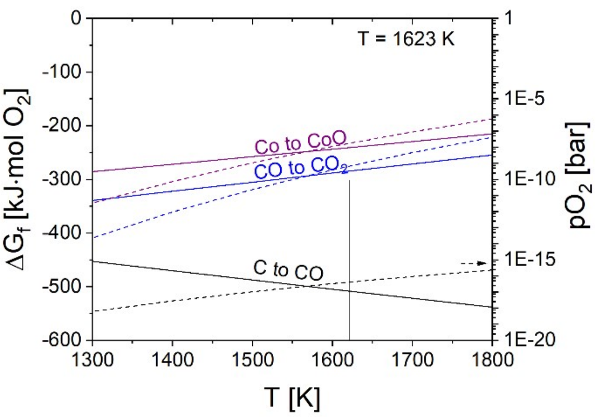

Figure S2: Calculated standard Gibbs free energies of oxide formation for cobalt and carbon (full lines), based on data from Barin et al.[48] and the corresponding equilibrium oxygen pressures (dashed lines).

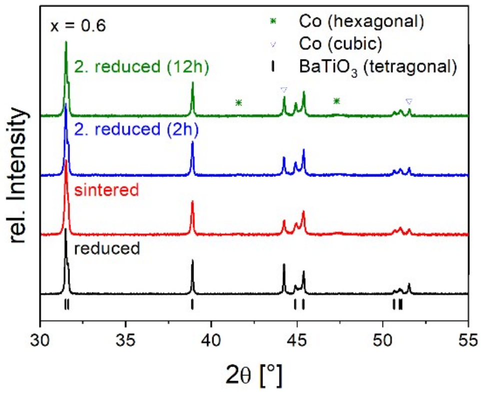

Figure S3: XRD patterns of $Co_{0.6}/(BaTiO_3)_{0.4}$ after reducing in forming gas at 1073 K for 2 h, sintering in nitrogen at 1623 K for 2 h with carbon as oxygen getter and after a further reductive sintering in forming gas at 1073 K for 2 or 12 h.

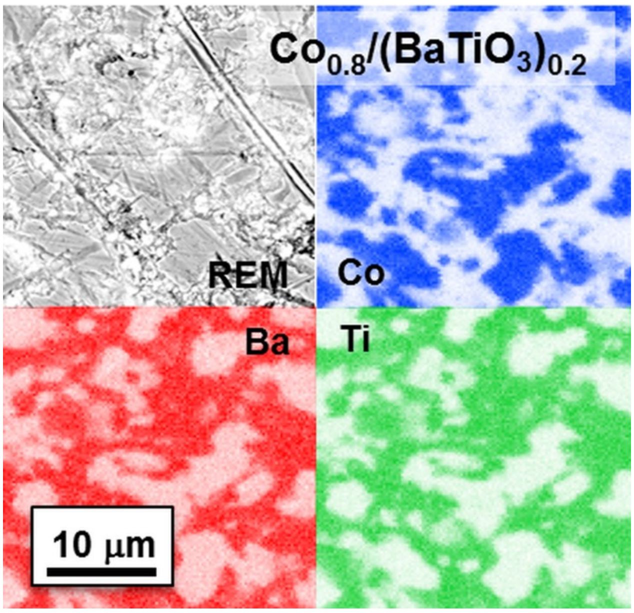

Figure S4: REM and EDX area scan of $Co_{0.8}/(BaTiO_3)_{0.2}$.

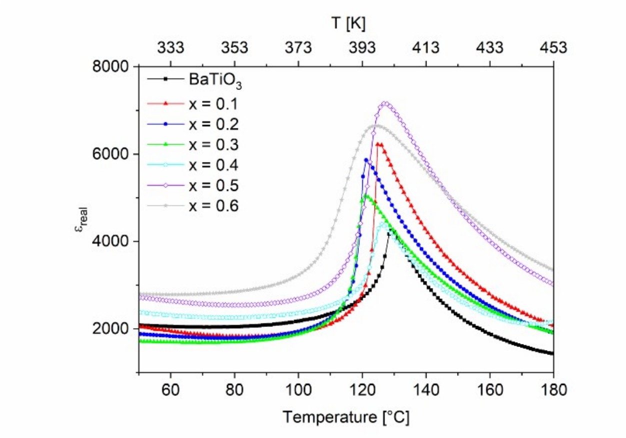

Figure S5: Temperature dependence of the relative permittivity of $Co_x/(BaTiO_3)_{1-x}$ with x = 0.1 to 0.6 measured at 1 kHz.

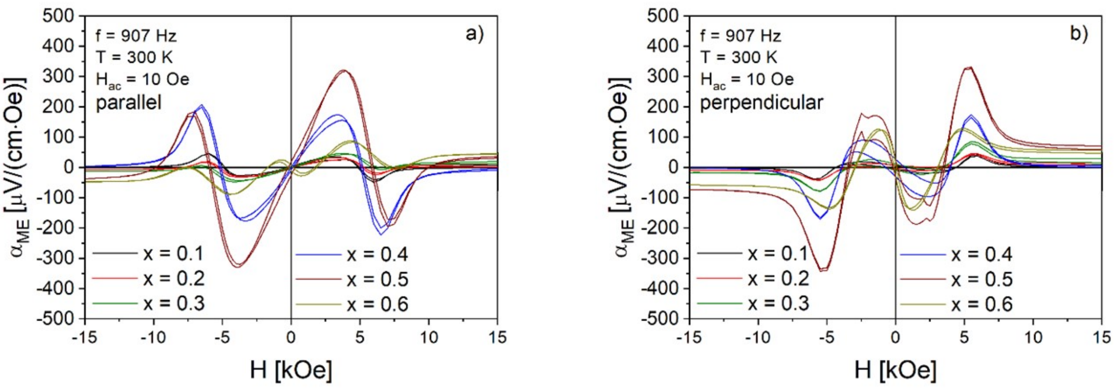

Figure S6: Field dependence of the magnetoelectric coefficients of the $Co_x/(BaTiO_3)_{1-x}$ samples (x = 0.1 to 0.6) for parallel (a) and perpendicular orientation (b).

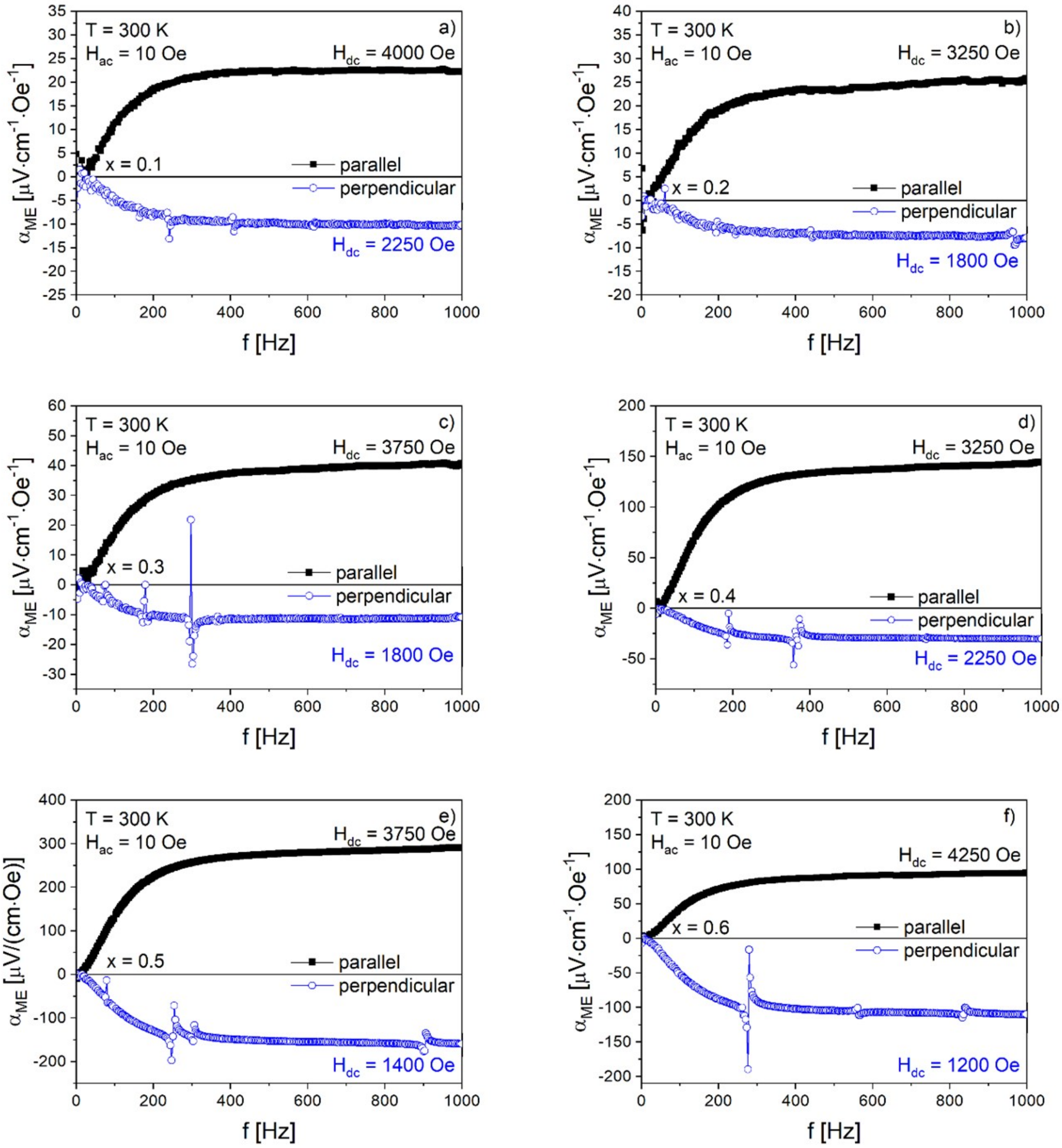

Figure S7: Influence of the frequency of the magnetic AC-field on α_{ME} for $Co_x/(BaTiO_3)_{1-x}$ samples with x = 0.1 (a), 0.2 (b), 0.3 (c), 0.4 (d), 0.5 (e) and 0.6 (f) in parallel (black filled squares) and perpendicular orientation (blue open squares).

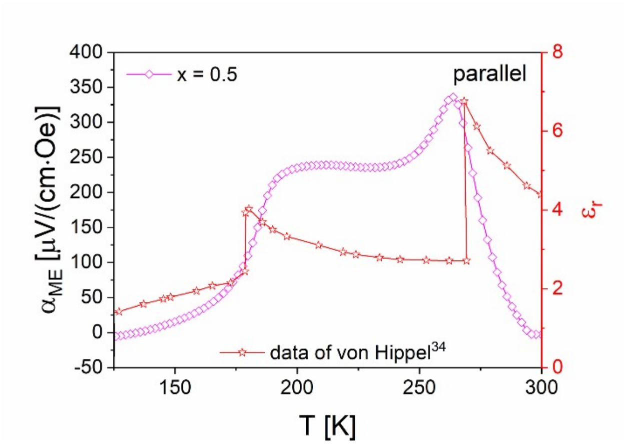

Figure S8: Temperature dependence of the magnetoelectric coefficient of the $Co_{0.5}/(BaTiO_3)_{0.5}$ composite in comparison with the dielectric constant of $BaTiO_3$ (according von Hippel[34]).

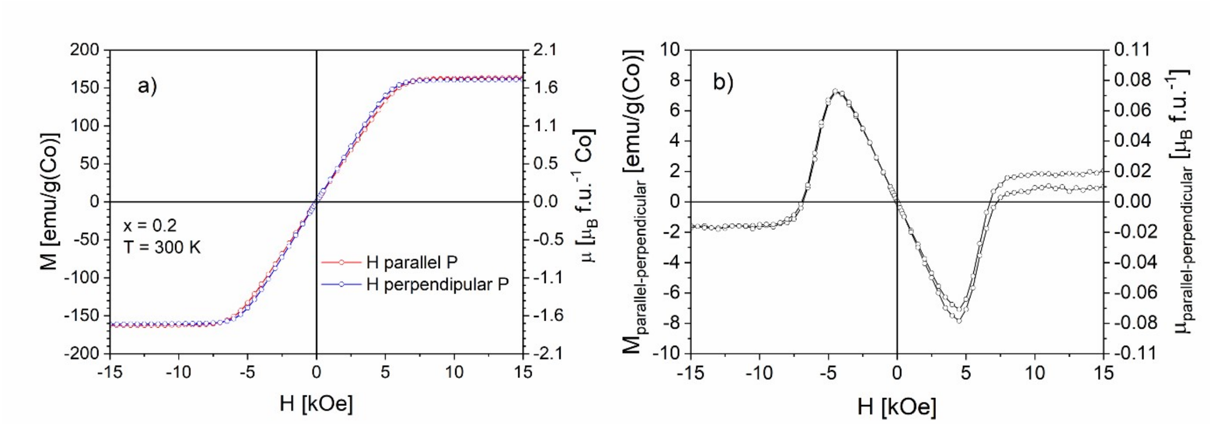

Figure S9: Comparison of M vs. H for an P∥H and P⊥H electrically poled $Co_{0.2}/(BaTiO_3)_{0.8}$ composite (a) and the difference between the observed magnetizations as a function of the magnetic field (b).